Infrared investigation on ice VIII and the phase diagram of dense ices

M. Song
Core Research for Evolutional Science and Technology, Japan Science and Technology Corporation, Kawaguchi, Saitama 332-0012, Japan

H. Yamawaki, H. Fujihisa, M. Sakashita, and K. Aoki*
National Institute of Advanced Industrial Science and Technology, Tsukuba Central 5, Tsukuba 305-8565, Japan
(Received 17 December 2001; revised manuscript received 31 January 2003; published 16 July 2003)

The phase diagram of the dense ices VII, VIII (molecular phases), and X (nonmolecular phase) was investigated over a *P-T* region of 12-298 K and 2-100 GPa by infrared absorption measurements. The ice VII-VIII and VIII-X phase boundaries determined in this study agree with those provided by previous Raman studies. The ice VII-X and VIII-X transitions can be characterized by the completion of rotational to distortional mode conversion (the disappearance of the ν_R rotational peak), and the ice VII-X boundary was determined accordingly. Triple points among the three phases are located at 100 K/62 GPa and 100 K/75 GPa for H_2O and D_2O ice, respectively. Substitution of hydrogen with deuterium pushes the boundary between the molecular (VII, VIII) and nonmolecular (X) ice phases toward higher pressures by 12–14 GPa, indicating clearly isotope effect on the phase transition due to dynamical translational disordering. Careful observation of infrared spectra near the triple point reveals that translational proton transfer arising from thermal activation and mutisite disordering becomes significant over a pressure span of about 10 GPa prior to the determined ice VII-X boundary. The frequency of the bending mode shows an anomalous softening below 8 GPa in both ice VII and ice VIII as a result of structural relaxation.

DOI: 10.1103/PhysRevB.68.014106 PACS number(s): 64.70.Kb, 62.50.+p, 78.30.−j, 63.20.Dj

I. INTRODUCTION

The phase diagram of ice simplifies at pressures above 2 GPa into two molecular phases, ice VII ($Pn3m$) with a body-centered-cubic (bcc) oxygen sublattice and ice VIII ($I4_1/amd$) with a slightly tetragonally distorted bcc oxygen sublattice. It has been predicted that the molecular phases VII and VIII transform into nonmolecular ice X ($Pn3m$) at higher pressures.[1] Water molecules are rotationally disordered in ice VII, whereas they are regularly oriented in an antiparallel configuration in ice VIII.[2] There exist two regimes of ice X, translationally disordered ice X (ionized phase) and fully centered ice X (atomic phase).[3–7] In the translationally disordered ice X, protons occupy the two stable sites along the hydrogen bond with equal probability due to tunneling effect. Further increase in pressure leads to a gradual conversion into the fully centered ice X in which the protons are located exactly at the bond midpoints. The dense ices VII, VIII, and X have closely related crystal structures and are satisfactorily described in terms of the static location or dynamic motion of the protons (deuterons) within the bcc or slightly distorted bcc oxygen lattices.

The phase transitions among these dense ices have been studied beyond 100 GPa, using both optical and x-ray techniques. The first Raman measurements of ice for pressures up to 100 GPa revealed that the VII-VIII boundary remains at 273 K up to 12 GPa and then rapidly decreases toward 0 K at approximately 60 GPa.[8] This boundary possibly merges into the ice VIII–translationally disordered ice X phase boundary (the ice VIII-X boundary) in the high pressure region around 60 GPa.[9–11] The transitions into the nonmolecular ionized and atomic phases has been investigated by x-ray diffraction,[12–14] precise analysis of the equation of state,[15,16] infrared absorption and reflection measurements,[17–22] and recently, by the Raman scattering.[23] The fully centered ice X with one Raman-active and two IR-active lattice modes has been observed at pressures above 100 GPa.[18,19,23] Quantum mechanical simulations of the x-ray diffraction spectra further indicated that the transition into the fully centered ice X occurs at around 110 GPa at 300 K.[6] Significant optical and x-ray diffraction signals were observed around 60 GPa, indicating possibly a transition into the translationally disordered ice X. Isotopic substitution by deuterium significantly shifts this transition to higher pressures by about 10 GPa. The ice VIII-X boundary,[9] thus far determined principally by the Raman measurement, is at approximately 62 GPa for temperatures below 100 K, a value obtained consistently in these studies. However, the reported pressure values for the VII-translationally disordered ice X transition (the ice VII-X transition, see Ref. 9) at ambient temperature range between 58 and 70 GPa, depending on the experimental and analysis methods used.[13–15,18–21] IR investigation on the ice VII-VIII and VII(VIII)-X transitions was not performed till now at variable temperature.

Further investigation of the phase transitions among the dense ices is necessary in order to determine some essential features of the phase diagram, such as the VII-X phase line, the triple point (if it exists) among phases VII, VIII, and X, and the isotope effects on the phase transitions. The transition from molecular ices VII and VIII into nonmolecular ice X is dominated by proton motions along hydrogen-bonded O-O axis. Probing this phase transition in fully ordered ice VIII is more effective than in orientationally disordered ice VII. Theoretical calculations on hydrogen-bond symmetrization or centering in dense ice have also been performed mainly for ice VIII at low temperatures. In ice VII, interfer-

ence from orientation and site disordering, and from temperature effects, may prevent clear observation of the ice VII-X transition. Detailed experimental investigations on ice VIII and the ice VII-VIII and VIII-X transitions, using experimental techniques capable of probing the positions and motions of protons, should be crucial for characterizing the ice VII-X phase transition and understanding the mechanism of hydrogen-bond centering in dense ice.

We measured infrared absorption spectra for H_2O and D_2O ices over the wide P-T range of 2–100 GPa and 12–298 K. Our purpose is to characterize the phase transitions among ices VII, VIII, and X, and finally to construct the phase diagram of dense ices. IR absorption measurements enable us to investigate the molecular and lattice vibrations related to protonic motions and hence to characterize the transitions among ices VII, VIII, and X more precisely. Interest is focused on the transitions from molecular to nonmolecular phase. The phase transition from the translationally disordered to the fully centered ice X occurs at around 110 GPa,[6] hence the ice X observed in the present study is, in fact, the translationally disordered ice X. Special effort was made to investigate the vibrational properties of ice VIII over the wide pressure range of 2–60 GPa at low temperatures. Our detailed comparison of ices VII and VIII reveals the differences in structural and bonding properties of these two phases that arise from ordering or disordering of molecular orientation.

II. EXPERIMENTAL DETAILS

High-pressure and low-temperature IR spectra were measured for a thin ice film prepared and pressurized in a membrane diamond-anvil cell (MDAC) made of CuBe. An ice film approximately 1 μm thick was prepared by depositing water vapor onto a disc of KBr pressure medium that filled the most volume of sample chamber. The dimensions of the sample chamber were approximately 50–60 μm in diameter and 30–40 μm in height. KBr pressure medium is transparent over a wide wave number range above 500 cm^{-1}, and hence does not interfere with the spectral measurement of ice. Sample preparation was performed in an MDAC cooled in advance to roughly 260 K with liquid N_2 in an N_2-purged glove box. The closed MDAC was then warmed to ambient temperature and mounted in a cryostat with KBr optical windows.

The cell was placed into a round copper holder attached to the cold tip of the cryostat and cooled in vacuum conditions of $10^{-6}-10^{-7}$ Torr. A resistive heater and diode thermal sensor for controlling and monitoring temperature were placed on the cold tip just above the MDAC holder. Sample temperature was measured with an Au+0.07%Fe-Cr thermal-couple fixed on the surface of one diamond anvil with stycast cement. Sample pressure was controlled by regulating the gas pressure in the membrane, and determined by following the method previously reported on the basis of a quasihydrostatic ruby scale.[24,25] Zero-pressure reference spectra at low temperatures were measured *in situ* with ruby balls fixed to the back surface of one diamond anvil. A few micrometer-sized ruby balls (about 5–8 μm in diameter) were scattered randomly inside the cell so as to estimate pressure distribution and determine the average pressure. The measured sample area was trimmed with an adjustable optical mask to a square of about 30 μm$\times$30 μm. IR spectra that were measured for both an empty MDAC at ambient pressure and for a KBr-filled MDAC at high pressures were used for correction of the diamond absorption. An FT-IR spectrometer with a focusing optics (magnification 10 and working distance 40 mm for each reflecting objective) was used for high-pressure and low-temperature spectral measurements with the MDAC contained in the cryostat. Spectra were collected in the wave number range of 650–6700 cm^{-1} with a 4 cm^{-1} resolution by 800 times accumulation.

In this study, over 20 experimental runs were conducted along either isothermal or approximately isobaric paths in order to precisely determine the phase boundaries in the pressure and temperature ranges of 2–100 GPa and 12–298 K.

III. RESULTS AND DISCUSSION

The crystal structure of ice VIII belongs to the space group $D_{4h}^{19}-I4_1/amd$. Group theory analysis of the vibrational modes predicts six IR-active modes:[26] two stretching modes [symmetric $\nu_1(A_{2u})$ and asymmetric $\nu_3(E_u)$], one bending mode [$\nu_2(A_{2u})$], two rotational modes [here termed the high- and low-frequency rotational modes $\nu_R(E_u)$ and $\nu_{R'}(E_u)$, respectively], and one IR-active translational mode [$\nu_T(E_u)$]. Normal mode analysis is not available for ice VII, which has a cubic structure with rotationally disordered molecules. However, the absorption bands observed for ice VII can be assigned on analogy with the mode assignments for ice VIII, as presented in previous studies.[20,21,27] For the fully centered ice X with a Cu_2O cuprite structure (O_h-Pn3m), two vibrational modes related to a lattice distortional motion, $\nu_D(E_u)$, and a translational atomic motion, $\nu_T(E_u)$, are predicted to be IR active.[18,19] The phase transitions among the high-pressure dense ices are identified here using these well-established spectral features.

A. VII-VIII transition

The top panel of Fig. 1 shows the spectral changes that occur during the VII-VIII transition at 6.5 GPa for decreasing temperatures in the range 298–258 K. The doublet located at 1500–1600 cm^{-1} in the 298 K spectrum, which is a resonant state between the ν_2 bending and $2\nu_{R'}$ overtone modes, responds sensitively to the ordering of molecular orientation that occurs in the VII-VIII transition. As the temperature decreases from 270–268 K, the lower frequency peak of the doublet shows an abrupt increase in intensity and a frequency shift from 1535 to 1500 cm^{-1}. This peak, centered at 1500 cm^{-1}, is assigned as the ν_2 bending mode of ice VIII. The transition temperature is determined to be approximately 269 K from the abrupt intensity increase and peak shift that occurs between 270 and 268 K. At the higher pressure of 22 GPa, obvious spectral change is also observed in the bending vibrational region (Fig. 1, bottom panel). The ν_2 bending peak of ice VIII appears at 1480 cm^{-1} at 239 K,

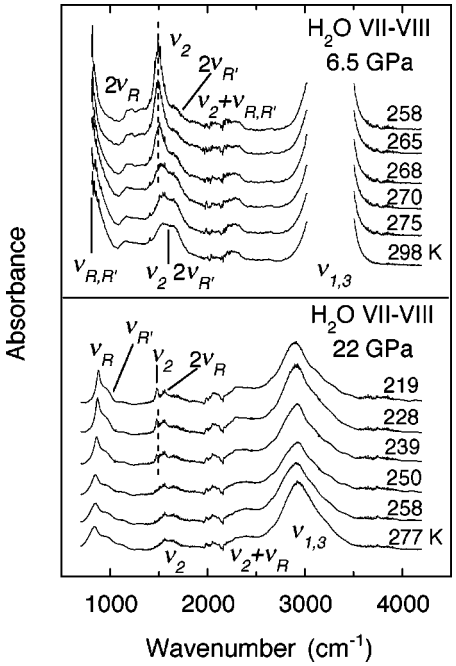

FIG. 1. IR absorption spectra of H_2O ice for isobaric paths at 6.5 GPa and 22 GPa across the VII-VIII transition. The spectra were collected during the cooling process. In the top panel, the $\nu_{1,3}$ stretching peaks with saturated absorbance are located in the 3000–3500 cm^{-1} range. The ν_2 bending peak exhibits a shift to low frequency in association with the VII-VIII transition. Dashed lines show the position of the ν_2 bending peak in ice VIII.

separated by about 100 cm^{-1} from the position of the ν_2 bending peak of ice VII at approximately 1570 cm^{-1}. The difference in the bending frequency is likely interpreted in terms of molecular dipole interaction and will be discussed again in the following subsection. The molecular $\nu_{R,R'}$ rotational peaks at approximately 800 cm^{-1} also show significant changes in peak width and intensity. They become sharp and intense with the transition into ice VIII. According to these spectral changes, the transition temperature at 22 GPa can be located at approximately 245 K, some 20 K lower than that determined at 6.5 GPa.

The temperature effect on the frequencies of the vibrational modes of ices VII and VIII was found to be negligible. A comparison of their peak frequencies helps us characterize the ice VII-VIII transition more directly. Figure 2 shows the frequency variations of the IR modes with pressure for ices VII and VIII. Except for the ν_2 bending mode, the corresponding modes in ice VII and VIII have nearly identical frequency-pressure curves over the measured pressure range, each showing a monotonic increase in frequency. Thus, the ordering or disordering of molecular orientation does not significantly affect these vibrational properties. In contrast, the ν_2 bending frequency is insensitive to pressure but the position of its absorption peak in ice VII is clearly different to its position in ice VIII (by about 100 cm^{-1} above 10 GPa) over the whole pressure range; this difference is probably related to multi-site disordering in the $\langle 111 \rangle$ directions in ice VII.[28] The ν_2 bending mode appears therefore to be sensitive to

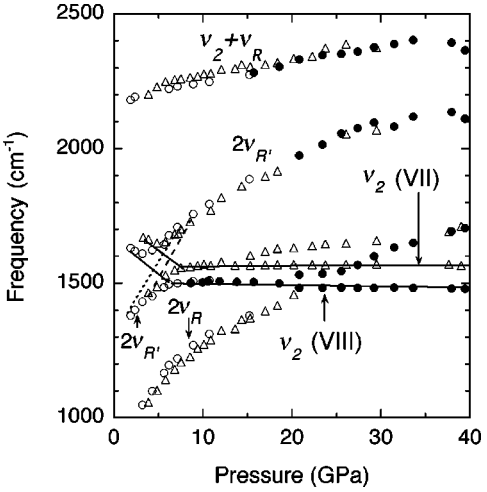

FIG. 2. Variations of the peak frequencies with pressure for H_2O ices VII and VIII in the pressure range 2–40 GPa. Solid circles are the frequencies of ice VIII at 60 K; open circles are those of ice VIII at 220–260 K; triangles are the frequencies of ice VII at 298 K. Solid and dashed lines approximately indicate the bare frequencies of the ν_2 bending and overtone $2\nu_R$ modes, respectively. The ν_2 bending mode exhibits an anomalous softening at pressures below 8 GPa.

molecular ordering and disordering, providing a sensitive probe of the ice VII-VIII transition.

The ice VII-VIII transition was mostly investigated here along isobaric warming and cooling paths. The variation of peak frequency or intensity with temperature enabled us to determine the transition temperature more accurately. Peak width also provides a precise indicator of the transition. The transition temperatures were thus determined from the plotting of peak frequencies and/or peak profile parameters as a function of temperature, although these plots are not shown here. The VII-VIII transition was found to take place reversibly with respect to temperature variation, with a hysteresis of 6-8 K at pressures up to 30 GPa, in agreement with previous results.[8,28]

B. Structural relaxation in ices VII and VIII

An anomalous softening of the ν_2 bending mode in ice VIII is observed below 8 GPa, as marked by the solid lines in Fig. 2. Although the softening behavior is indistinct because of frequency modulation due to mode mixing with the $2\nu_{R'}$ overtone modes (Fig. 3), the unperturbed frequency of the ν_2 bending mode (obtained by Fermi resonance analysis) in ice VIII is found to decrease from 1650 cm^{-1} at 2.0 GPa to 1500 cm^{-1} at 7.7 GPa. The softening of the ν_2 bending mode can be interpreted in terms of structural relaxation; the separation between two interpenetrating sublattices in ice VIII was observed to increase from 19 pm at 7 GPa to 25 pm at about 1 GPa during pressure releasing at low temperatures by neutron diffraction measurements.[29–31] Structural relaxation, possibly driven by repulsive dipole-dipole interactions, occurs through a sudden movement of interpenetrating sublattices in opposite directions[29–31] and also through an anomalous increase in the bond angle of the water molecules.[31]

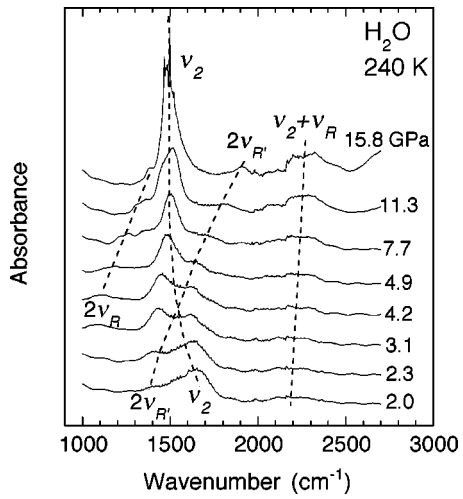

FIG. 3. IR absorption spectra of H_2O ice VIII at 240 K, measured during the unloading process. The pressure variations of peak intensity observed for the ν_2 and $2\nu_R$ modes are attributed to mode mixing (Fermi resonance) between the two modes. The ν_2 frequency shows softening behavior up to 8 GPa, becoming pressure insensitive at higher pressures. Dashed lines are guides only.

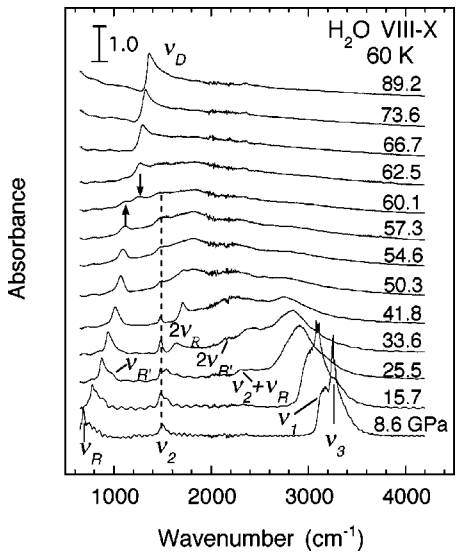

FIG. 4. IR absorption spectra of H_2O ice for a 60 K isothermal compression run up to 89 GPa. A distinct spectral change is observed in the rotational region around 1200 cm^{-1} at approximately 60 GPa (marked by short arrows), interpreted here as a vibrational mode conversion associated with the VIII-X transition. The ν_2 bending peak remains at approximately 1500 cm^{-1} for pressure increases up to 60 GPa (dashed line).

An anomalous softening was also observed for the Raman-active $\nu_1(A_{1g})$, $\nu_1(B_{1g})$, and $\nu_3(E_g)$ stretching modes at rather low pressures below 2 GPa.[29] Based on the correlation between decoupled O-H vibrations and the hydrogen bond length,[32,33] the softening of Raman-active stretching modes arises from a rapid decrease of the hydrogen-bonded O-O distance with pressure. This softening can hence be characterized as a short-distance interaction. By contrast, that of the ν_2 bending mode is attributed to the interaction between the bending motions and crystal fields originating from the molecular dipole moments. Such long-distance interactions may be responsible for the softening of the ν_2 bending mode over a wide pressure span.

It is significant that the ν_2 bending mode exhibits the softening behavior even in ice VII with its water molecules rotationally disordered (see Fig. 2). The crystal structure of ice VII consists of interpenetrating sublattices, as is also true of ice VIII. The water molecules in each sublattice of ice VII are disordered in orientation, in contrast to their regular orientation in ice VIII. If the molecules in ice VII were fully disordered, the repulsive dipole-dipole interaction between the sublattices would vanish and structural relaxation would be prevented. It is probable that middle range ordering in molecular orientation is preserved in ice VII. The *Ice rule* forbids fully disordered molecular orientation in a hydrogen-bonded network, requiring formation of antiferroelectric domain structures even in disordered ice VII. The crystal field due to the molecular dipole moments likely influences the ν_2 bending vibration significantly in ordered ice VIII, but not in disordered ice VII. In ice VII the long-range ordering in molecular orientation or dipole moment is lost and consequently the average dipole moment becomes 0. The interaction between the crystal field and the vibrational motion may explain the frequency difference (about 100 cm^{-1}) between ices VII and VIII.

C. VIII (VII)-X transition

1. VIII-X transition in H_2O ice

The transition from phase VIII to phase X was investigated by isothermal compression at temperatures below 100 K. Figure 4 shows a representative spectral set for a 60-K isothermal run in the pressure range of 8–90 GPa. The spectrum of ice VIII at 8.6 GPa exhibits three molecular peaks, which are related to the asymmetric ν_3 and symmetric ν_1 stretching vibrations, and to the bending ν_2 vibration, observed at approximately 3300, 3150, and 1500 cm^{-1}, respectively. In addition, the peak arising from the fundamental rotational vibrations and its overtone and combination bands are observed more clearly at higher pressures, around 30–40 GPa. Each molecular vibrational mode shows characteristic pressure behavior. The stretching peaks rapidly shift to low frequency with increasing pressure, whereas the rotational peaks shift to high frequency. By contrast, the bending peak is insensitive to pressure, staying at approximately the same position for all pressures up to 60 GPa.

The peak frequencies for ice VIII at 60 K are plotted as a function of pressure in Fig. 5. The splitting of the ν_1 and ν_3 stretching peaks, which is not observed for ice VII, is observed for ice VIII up to 22 GPa. As the pressure is increased, the $\nu_{1,3}$ stretching modes are found to mix successively with the $\nu_2+\nu_{R,R'}$ combination and $2\nu_{R'}$ and $2\nu_R$ overtones, while their frequencies decrease from approximately 3300 cm^{-1} at 5 GPa to about 1000 cm^{-1} at 60 GPa. The frequencies are most significantly perturbed at approximately 30, 40, and 48 GPa due to the mode mixing, avoiding frequency crossing (Fermi resonance).[20,21] The unperturbed frequencies are obtained for each vibrational mode by following the fitting procedure described in previous

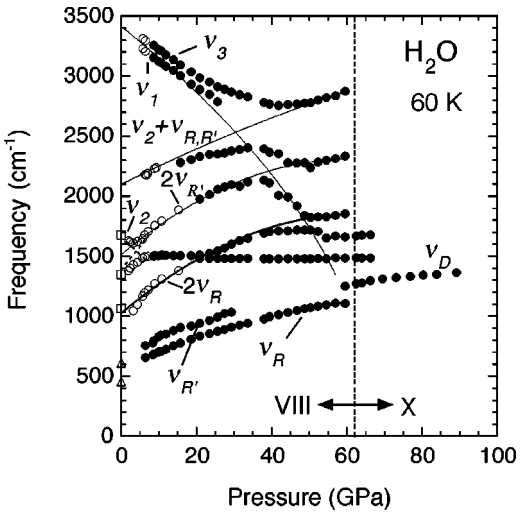

FIG. 5. Variation of the peak frequencies with pressure measured for H_2O ice VIII. Solid circles represent the peak frequencies measured by 60 K runs and open circles represent by 200–260 K runs. Open squares and triangles are those referred from Ref. 34 and Ref. 35, respectively. The stretching frequency is described as a function of pressure by $\omega_{OH}=(\omega_0^2-aP)^{1/2}$, here $\omega_0=3415$ cm^{-1} and $a=1.73\times10^5$ cm^{-2}/GPa, with which a critical pressure Pc of 67.5 GPa is obtained for $\omega_{OH}=0$. The frequencies of the other modes are fitted by a quadratic expression in pressure P, $\omega=a+bP+cP^2$; $a=2100$ cm^{-1}, $b=15.6$ cm^{-1}/GPa, and $c=-0.04$ cm^{-1}/GPa^2 for the $\nu_2+\nu_{R,R'}$ mode, $a=1515$, $b=26.1$, and $c=-0.22$ for the $2\nu_{R'}$ mode, $a=1027$, $b=26.3$, and $c=-0.21$ for the $2\nu_R$ mode, $a=657$, $b=18.2$, and $c=-0.19$ for the $\nu_{R'}$ mode, and $a=574$, $b=13.9$, and $c=-0.08$ for the ν_R mode.

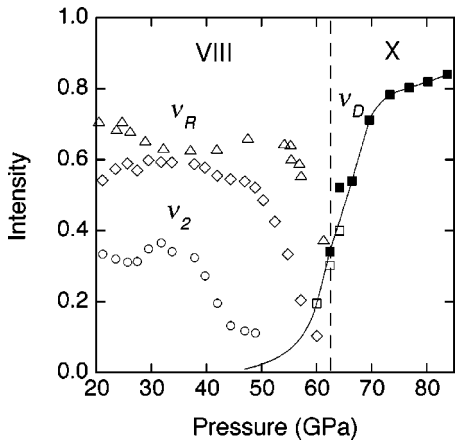

FIG. 6. Variation of the peak intensities of the ν_2 bending, ν_R rotational and ν_D distortional modes in H_2O ice with pressure. Open triangles are the data obtained at 20 K, other symbols are for 60 K. Open symbols are fitted data and solid symbols are peak heights read directly from the spectra. The intensities of the ν_2 and ν_R modes, which are approximately constant at low pressure, begin to decrease at approximately 40 GPa and 50 GPa, respectively. In contrast, the ν_D mode, which begins to appear near 60 GPa, shows a monotonic increase in intensity with pressure. Solid line is the guide for the ν_D mode only.

papers,[10,20] and are presented as solid lines in Fig. 4. The frequency of softening $\nu_{1,3}$ stretching modes is described as a function of pressure by a phenomenological function $\omega_{OH}=(\omega_0^2-aP)^{1/2}$, with a critical pressure P_c of 67.5 GPa for $\omega_{OH}=0$. However, the soft-mode analysis of the stretching frequency, which is based on a harmonic approximation and is effective at low pressure, provides only an approximate estimation on the location of the ice VIII(VII)-X transition. A theoretical investigation on the vibrational property of dense ice has explicitly demonstrated the breakdown of the harmonic approximation due to the anharmonicity of proton or deuteron motion towards hydrogen-bond centering.[36]

The significant spectral change of the ice VIII-X transition is observed at approximately 60 GPa (Fig. 4), including a peak alternation due to the associated structural change. The molecular vibrational peaks broaden significantly with increasing pressure and so provide no detectable indication of the transition. However, the spectra show distinct change in the wave number range of 1100–1300 cm^{-1}; the rotational peak ν_R at approximately 1100 cm^{-1} disappears above 62.5 GPa, while a new peak at approximately 1250 cm^{-1} appears at the slightly lower pressure of 60.1 GPa. This new peak grows in intensity with further increase in pressure, showing asymmetric shape even at 89.2 GPa due to the Fano interference[17] and symmetrically sharpened shape above 100 GPa eventually. The peak sufficiently sharpened at higher pressure corresponds to the lattice distortional mode ν_D of the fully centered ice X with a Cu_2O cuprite structure, which is a distortional twisting vibration of the tetrahedron of hydrogen atoms around a stationary oxygen atom.[18,19]

The observed spectral change can be related to a sequential transition from the molecular to atomic phase via an intermediate translationally disordered or ionized state. According to the correlation diagram for the vibrational modes of ice VIII and the fully center ice X, the rotational modes (ν_R and $\nu_{R'}$) of ice VIII are predicted to convert into the distortional lattice mode (ν_D) of ice X in association with the transition.[26] As indicated by the intensity variations of the ν_R rotational and ν_D distortional peaks with pressure (Figs. 4 and 6), a rotational-distortional mode conversion was observed at around 60 GPa. This mode conversion, however, is interpreted to result from translational proton tunneling, which allows formation of the tetrahedron of hydrogen atoms and therefore the appearance of the ν_D distortional mode in the translationally disordered ice X. The spectral change around 60 GPa is, therefore, attributed to the ice VIII-X transition and the transition pressure at 60 K is determined to be 62.5 GPa by the completion of rotational-distortional mode conversion featured by the disappearance of the ν_R rotational peak at around 1100 cm^{-1} (see Figs. 4 and 6). In the translationally disordered ice X, the ν_D distortional peak becomes the main vibrational peak over the whole frequency range. A highly broadened band with a maximum height around 1600 cm^{-1}, which the original bending and stretching peaks merge into, remains even after the low-pressure rotational peak has disappeared (see the 62.5 GPa spectrum). This band may involve several peaks related to the molecular vibrations of neutral and ionized water molecules: H_2O, hydroxyl anions OH^-, and hydro-

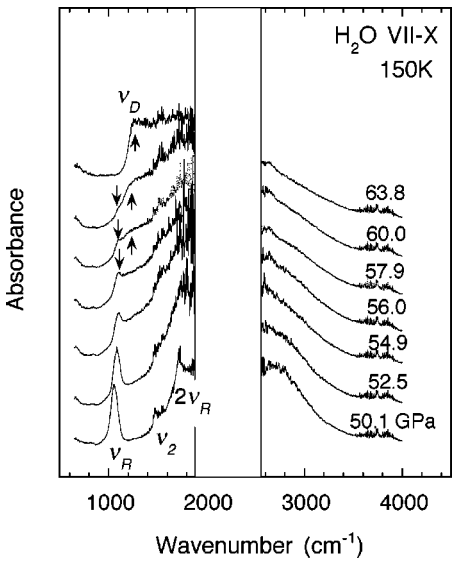

FIG. 7. IR absorption spectra of H_2O ice for a 150 K isothermal compression up to 63.8 GPa. Disappearances of the ν_2 bending and ν_R rotational peaks at around 52.5 and 60 GPa, respectively, are attributed to successive transitions from ice VIII to ice VII and further to ice X. Absorption from the diamond anvils interferes with spectral measurements for the wave number region from 2000 to 2600 cm^{-1} (blank region).

nium cations H_3O^+. Theoretical calculations have predicted 25% ionization of water molecules as a result of enhanced proton tunneling, giving rise to a intermediate ionized state between the molecular and atomic phases at these pressures.[3,37] Further compression leads the ν_D distortional peak to become sharpening and symmetric gradually and the fully centered ice X was finally realized at pressures above 100 GPa.[6,18,19,23]

2. VII-X transition in H_2O ice

The VII-X transition was investigated at several fixed temperatures above 100 K on compression across the phase boundary, which is located at approximately 60 GPa. Figure 7 shows the absorption spectra collected during a pressure increase from 50 to 64 GPa at 150 K. The spectrum at 50.1 GPa, with three sharp peaks located on significantly broadened stretching bands, is identified as that of ice VIII. A small increase in pressure by 2–3 GPa results in a small shift of the rotational peak toward higher frequencies and also in the disappearance of the sharp ν_2 and $2\nu_R$ peaks, due to the proton disordering associated with the transition into ice VII. Further compression causes peak alternation at 60 GPa in a manner similar to that observed for the VIII-X transition. The ν_D distortional peak is already recognizable in the 57.9 GPa spectrum, while the ν_R rotational peak is no longer evident in the 63.8 GPa spectrum. The VII-X transition pressure is estimated to be 61.9 GPa on the basis of the same criterion as used for the ice VIII-X transition. Ice VII is present over a narrow pressure range of about 10 GPa at 150 K prior to the transition into nonmolecular ice X.

Both the ice VII-X transition and the ice VIII-X transition are characterized by the completion of rotational-distortional mode conversion, enabling the determination of the phase boundaries. The observation in the present study of this common IR feature for the ice VII-X and VIII-X transitions is in agreement with previous speculations on the nature of the ice VIII(VII)-X transition, which is believed to involve proton or deuteron translational motion along the hydrogen-bonded O-O axis.[3–5] The mode conversion in the ice VII-X transition was observed previously at ambient temperature,[18] although its feature was not clear due to the peak broadening caused by disordering and the temperature effect. At low temperatures the peak broadening was significantly reduced and the transition pressures were able to be determined definitely from the disappearance of the rotational peak at 1100 cm^{-1} with the aid of the observation of the ice VIII(VII)-X transition.

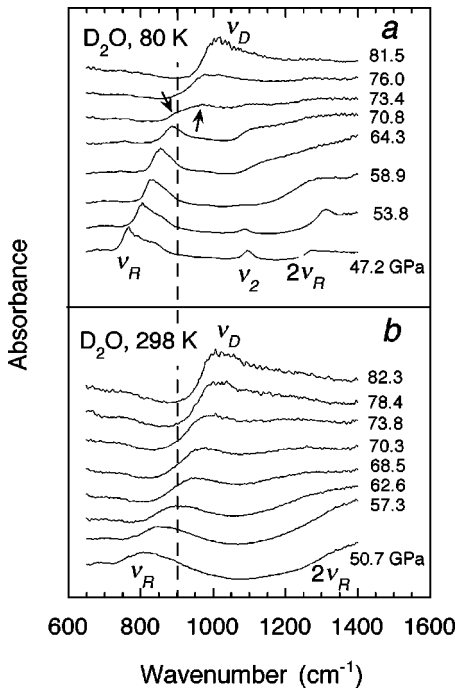

FIG. 8. IR spectra of D_2O ice measured along (a) 80 K isothermal and (b) 298 K isothermal paths in the pressure range of 47–83 GPa. In (a), the doublet at 800–1000 cm^{-1} in the 73.4 GPa spectrum can be divided into rotational and distortional peaks at 900 and 970 cm^{-1}, respectively. The rotational peak is no longer recognizable in the 76 GPa spectrum. In (b), the ν_R-ν_D mode conversion can not be clearly observed, so the ice VII-X transition pressure is estimated by analyzing the spectra around 70 GPa on the basis of the spectral features of the ice VIII-X transition.

3. VIII(VII)-X transition in D_2O ice

The characteristics of these phase transitions for D_2O ice are the same as those for H_2O ice except for the isotope effect on vibrational mode frequencies and phase transition pressures. Figure 8 presents two sets of spectra for D_2O ice, one showing the VIII-X transition at 80 K and the other the VII-X transition at 298 K. In Fig. 8(a), the distortional peak appears at 970 cm^{-1} in the 73.4 GPa spectrum, while the rotational peak at 900 cm^{-1} is still present at this pressure. A slight increase in pressure leads to the disappearance of this

rotational peak, as seen in the 76.0 GPa spectrum. The pressure of the ice VIII-X transition at 80 K is, therefore, 74.7 GPa, determined according to the observed rotational-distortional mode conversion. The rotational-distortional mode conversion can not be observed clearly in the spectra measured at 298 K, as shown in Fig. 8(b). On the basis of the observed spectral features of the ice VIII-X transition, we suggest that the spectral profile in the 850–1000 cm^{-1} region in the 68.5 GPa spectrum can be understood as a doublet composed of rotational and distortional peaks, similar to those at 73.4 GPa shown in Fig. 8(a). In the 73.8 GPa spectrum, the rotational component that should appear at around 900 cm^{-1} is unrecognizable. The ice VII-X transition at 298 K was hence estimated at 72.1 GPa.

D. Phase diagrams

The phase diagram of H_2O ice determined from the observed IR spectra is shown in Fig. 9(a). Some previously reported data[8,11,13,17–21,23] are also presented in this figure. The VII-VIII transition temperature, initially located at 273 K below 10 GPa, decreases from this value at approximately 15 GPa at an approximate rate of -3 to -4 K/GPa, producing a VII-VIII phase boundary in good agreement with that determined by the Raman measurements.[8,23] As described in the preceding section, careful measurement along the 150 K isotherm reveals that ice VIII transforms first into ice VII, and then into ice X with a further 10 GPa increase in pressure. However, at temperatures below 100 K, ice VIII transforms into ice X without entering the ice-VII field. The VII-VIII phase boundary thus merges into the VIII-X boundary via a triple point located approximately at 100 K and 62 GPa. The transition temperature from the molecular (VII or VIII) phases to the nonmolecular phase (X) tends to decrease rapidly with increasing pressure, giving an almost vertical boundary with a negative slope of -92 K/GPa. It should be noted here again that the nonmolecular phase located near the phase boundary is the translationally disordered ice X, which gradually transforms into the fully centered ice X on further compression.

As shown in Fig. 9(b), the phase diagram of D_2O ice is quite similar to that of H_2O. At pressures below 20 GPa, the VII-VIII phase boundary of D_2O ice is only about 4 K higher than the same H_2O-ice boundary, with minimal obvious influence from isotope effects. The transition temperature decreases with pressure at a rate of about -3 K/GPa, a rate which is only a little smaller than that of H_2O ice. Isotope effects on the phase transitions are most evident in the boundary between the molecular and atomic phases. The transition points on the boundary are located at 72 GPa/298 K and at 77 GPa/16 K, pressures that are 20–25 % higher than those for the H_2O-ice diagram. The phase boundary has a slight incline, with a slope of -57 K/GPa. The isotope effects on these transition pressures, especially for the VIII-X transition, have been investigated theoretically, and can be interpreted in terms of zero-point energy and tunneling probability, which leads to a significant shift of the VIII-X phase boundary toward higher pressure.[3,4] The phase boundary shift observed is in agreement with the theoretical predictions, showing that the molecular to nonmolecular phase transition is likely dominated by tunneling motion.[3–5,10,38] The triple point is located at approximately 100 K and 75 GPa, higher by 13 GPa than that determined for H_2O ice.

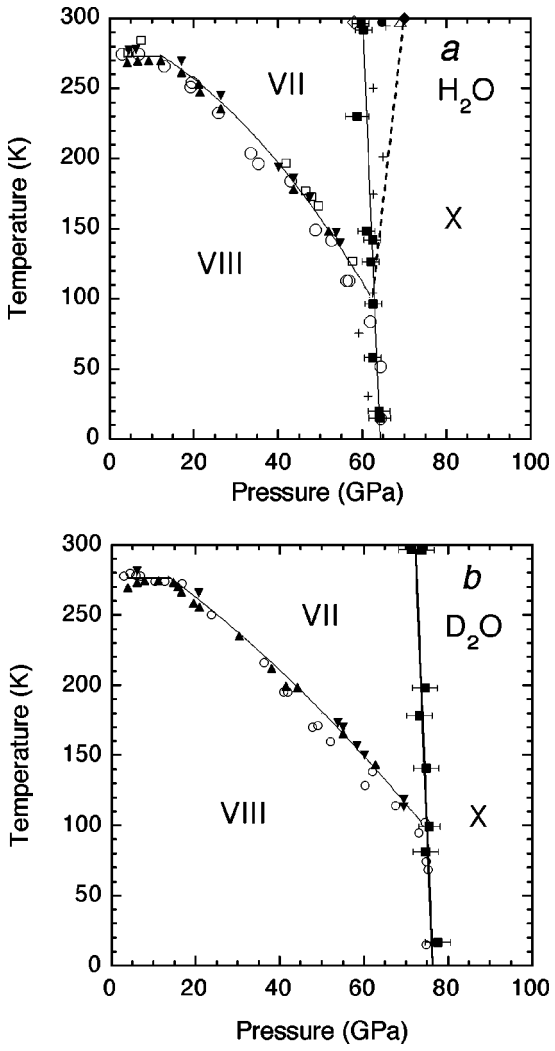

FIG. 9. Phase diagrams of H_2O (a) and D_2O (b) ices at low temperature and high pressure. Solid triangles ( ) and ( ) represent transition points determined by cooling and warming runs, respectively. Solid squares represent those determined by isothermal runs. The data previously reported are also presented by open circles (Ref. 8), an open triangle (Refs. 11 and 13), a solid circle (Ref. 19), a solid diamond (Ref. 20), an open diamond (Ref. 21), open squares and crosses (Ref. 23). The dashed line is the ice VII-X boundary proposed in previous studies (Refs. 11 and 23).

The ice VIII-X boundary determined by our IR measurements agrees with the previous Raman results.[8,10,11,23] We note that the most pronounced Raman signal of the ice VIII-X transition is the damping (also softening and broadening) of the two Raman-active translational $\nu_{Tz}(A_{1g}) + \nu_{Txy}(E_g)$ and $\nu_{Tz}(B_{1g}) + \nu_{Txy}(E_g)$ modes[23] related only to the vibrations of the oxygen sublattice.[34] In contrast, the IR signal of this transition used in the present study is the mode conversion of the IR-active ν_R rotational and ν_D distortional modes related to the protonic motion; the completion of the ν_R-ν_D conversion is interpreted to be a result of proton tun-

neling along the hydrogen-bonded O-O axis. From this perspective, IR spectroscopy is more effective for characterizing the ice VIII-X transition.

The ice VIII(VII)-X transition has also been investigated in previous IR experiments at both room and low temperatures (85–300 K),[18–22] and in x-ray diffraction experiments at room temperature.[12–14] Considerable effort was made in these studies to determine the pressure of the ice VII-X transition at room temperature, with the reported pressure values ranging from 58 to 70 GPa.[13–15,18–21] A soft-mode analysis of the IR-active stretching mode[20] and an analysis of the equation of state[13] yielded a pressure value of 66–67 GPa (about 70 GPa after being converted with the quasihydrostatic ruby scale[25]) for the VII-X transition at room temperature, several GPa higher than that determined from the discontinuity between IR-active ν_R rotational and ν_D distortional modes.[18,21] The IR measurements presented here reveal that both the ice VII-X and VIII-X transitions can be characterized by the completion of the rotational-distortional mode conversion, and that the harmonic approximation of a soft-mode analysis is not appropriate for determining the pressure of the ice VII-X transition because of the anharmonic nature of hydrogen-bond centering in dense ice. The phase boundary of the ice VII-X transition as determined by the present method is almost vertical with a negative slope, different to that previously proposed, which had a positive slope.[11,23]

Close to vertical VII, VIII-X phase lines imply that ices VII and VIII have crystal structures very close to each other and the phase lines are probably of the nature of translational proton tunneling effect, in which process is dominated by the hydrogen-bond length and the hydrogen-bonded O-O separation. As revealed by the neutron diffraction experiment up to 20 GPa, ice VII possesses a multisite disordered structure and at 5 GPa contains both 2.75 Å and 2.93 Å hydrogen-bonded O-O bond lengths, about 0.1 Å shorter or longer than that in ice VIII at the corresponding pressure.[28] Although the difference in bond length may be reduced from 0.2 Å with pressure, as little as 0.06 Å difference could account for a 15 GPa wide zone for the ice VII-X transition, with the center line of the transition zone being approximately at the same pressures as the ice VIII-X phase line. The IR features for the ice VII-X phase line determined in this study are closely the same as the ice VIII-X phase line, suggesting that the difference in bond length seems to vanish as the pressure approaches the VII-X phase line. However, the multisite disordering of ice VII do exist and affect translational proton transfer at pressures below the ice VII-X phase line as described in the following section.[28] The ice VIII-X transition around 62 GPa below 100 K is predicted to be accompanied by a structural change from a tetragonal to a cubic (bcc) lattice, which can not be verified by optical measurements. Further observation with structural tools such as x-ray and neutron diffraction techniques is still required for precise understanding of the molecular to nonmolecular transition in the dense ices.

E. Thermally activated proton transfer

Infrared observations of the ν_D distortional mode and of the rotational-distortional mode conversion provide insight into the process of hydrogen-bond centering in dense ice. The phase transition for H_2O ice at approximately 60 GPa can be interpreted as the transition from the molecular phases VII and VIII into the translationally disordered ice X. The fully centered ice X (atomic phase) has been found to appear at around 110 GPa,[6] which is far above the pressure of the ice VII(VIII)-translationally disordered ice X transition. It should be noted that the ν_D distortional peak, which is a definite signal for the fully centered ice X with the Cu_2O structure, is even observed for the translationally disordered ice X. Tetrahedrons of hydrogen atoms might be formed as a result of possible proton transfer along the hydrogen bond prior to the entire transition into the fully centered ice X.

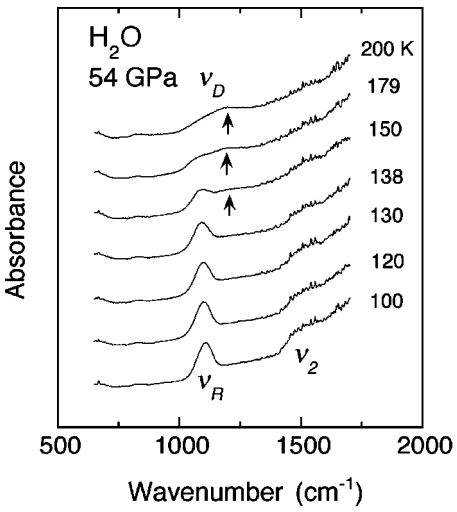

FIG. 10. IR spectra of H_2O ice at 54 GPa and 100–200 K. Ice VIII transforms into ice VII as the temperature increases from 138 to 150 K. The distortional peak near 1200 cm^{-1} (marked by arrows) becomes recognizable in the spectra of ice VII above 150 K. The ν_R and ν_D peaks for ice VII show an intensity exchange with increasing temperature.

Considering that the ν_D distortional mode is converted from the ν_R rotational mode, the intensity variations of the ν_D distortional and ν_R rotational peaks with pressure, especially the intensity decrease of the ν_R rotational peak above 50 GPa, indicate that the rotational-distortional mode conversion is possibly initiated at approximately 50 GPa (see Figs. 4 and 6). A convincing evidence for the existence of the rotational-distortional mode conversion in the pressure range of 50–60 GPa was obtained by heating ice from 100 to 200 K along a 54 GPa isobaric P-T path (Fig. 10). As the temperature increases from 138 to 150 K, ice VIII transforms into ice VII, with the ν_D distortional peak clearly appearing at approximately 1200 cm^{-1} in the 150 K spectrum. Further increase in temperature causes exchange in the peak intensity between the ν_R rotational and the ν_D distortional modes. The appearance of the ν_D distortional peak at approximately 50–60 GPa in ice VII implies that the protons can transfer between the two stable sites along the hydrogen bond to form tetrahedrons in this pressure range. We may relate qualitatively the peak intensity of the ν_D distortional mode to the proton transfer probability and hence the ν_D distortional peak at approximately 50–60 GPa is interpreted to result

from thermally activated translational proton transfer (hopping), which allows formation of the tetrahedron of hydrogen atoms. For ice VIII, the distortional peak is expected to be present at 1200–1300 cm^{-1} even at pressures of 50–60 GPa, however, the spectra show no obvious signal in the expected wave number region possibly due to low probability of thermally activated proton transfer in ice VIII.

The multisite-disordered structure for ice VII indicates that the covalent O-D(H) bond length in ice VII is identical to that in ice VIII but the hydrogen-bonded O-O separations in ice VII are a mixture of lengths about 0.1 Å longer or shorter than ice VIII.[28] As observed along the 54 GPa isobaric *P-T* path (see Fig. 10), the ν_D distortional peak is unrecognizable in the spectra of ice VIII below 150 K but is clearly observed in the 150 K spectrum as ice VIII transits into ice VII. This phenomenon can be attributed to the existence of the shorter hydrogen-bonded O-O separations in ice VII, and hence serves an evidence for the multisite-disordering model for ice VII. Even though the ice VII-X boundary is determined as a line at 60–62 GPa (72–75 GPa for D_2O ice), dynamical translational disordering, which arises from thermally activated proton transfer and multisite disordering, becomes significant in ice VII at pressures about several to 10 GPa below the determined ice VII-X boundary as indicated by the appearance of the ν_D distortional peak (Fig. 10).[6,28] The dynamical translational disordereing arising from thermallly activated proton transfer and multisite disordering below the determined ice VII-X boundary can also been taken as the onset of the ice VII-X transition although we generally denote the ice phase below the determined ice VII-X phase line as ice VII, and this is in agreement with a latest quantum mechanical calculation on dense ice at room temperature.

IV. SUMMARY

The infrared absorption spectra of H_2O and D_2O ices were measured for the wide *P-T* range of 2–100 GPa and 12–298 K. The phase transitions between ices VII, VIII, and X were satisfactorily characterized from the observed spectra, allowing a precise determination of the phase boundaries. The ice VII-X and VIII-X transitions are characterized by the completion of rotational to distortional mode conversion (the disappearance of the ν_R rotational peak), and the phase boundaries thus determined are in agreement with those previously reported.[8,18,21,23] The triple point is located at 100 K and 62 GPa for H_2O ice and at 100 K and 75 GPa for D_2O ice. Substitution of hydrogen with deuterium moves the boundary between the molecular (VII, VIII) and nonmolecular (X) ice phases toward higher pressures by 12–14 GPa, indicating clearly isotope effect on the phase transition related to dynamical translational disordering. The ice VIII(VII)-X boundry determined in this study is interpreted as a result of tunneling effect, which allows the formation of hydrogen tetrahedrons and hence the appearance of the ν_R distortional peak. Careful observation of infrared spectra near the triple point reveals that translational proton transfer arising from thermal activation and mutisite disordering becomes significant in ice VII over a pressure span of about 10 GPa prior to the determined ice VII-X boundary, especially at room temperature.[6] Thermally activated proton transfer may also exist in ice VIII at pressure above 50 GPa (about 65 GPa for D_2O ice), but the probability of proton transfer is low. Each vibrational mode of ice VII and the corresponding mode of ice VIII were found to have nearly equal peak frequencies over a pressure range of 2 GPa to at least 40 GPa. The ν_2 bending mode was an exception, showing a frequency difference of 100 cm^{-1} between the two phases, which is probably related to multisite disordering in the $\langle 111 \rangle$ directions in ice VII.[28] The ν_2 bending mode also showed unusual behavior with pressure; the peak position shifted to a lower frequency for pressures up to 8 GPa and remained at almost the same position upon further compression. This softening behavior of the ν_2 bending mode was interpreted to be a result of structural relaxation.

ACKNOWLEDGMENTS

We wish to thank Dr. Prudence Foster for kindly revising the manuscript. M.S. would like to thank Dr. Y. Matsushita, Dr. A. Nakayama, and E. Katoh for their assistance. This work was conducted under the Core Research for Evolutional Science and Technology (CREST) project supported by the Japan Science and Technology Corporation (JST).

*Author to whom correspondence should be addressed. Email address: k-aoki@aist.go.jp

[1] W.B. Holzapfel, J. Chem. Phys. **56**, 712 (1971).

[2] W.F. Kuhs, J.L. Finney, C. Vettier, and D.V. Bliss, J. Chem. Phys. **81**, 3612 (1984).

[3] K. Schweizer and F.H. Stillinger, J. Chem. Phys. **80**, 1230 (1984).

[4] M. Benoit, D. Marx, and M. Parrinello, Nature (London) **392**, 258 (1998).

[5] P.G. Johannsen, J. Phys.: Condens. Matter **10**, 2241 (1998).

[6] M. Benoit, A.H. Romero, and D. Marx, Phys. Rev. Lett. **89**, 145501 (2002).

[7] Translationally disordered ice X has been referred as translationally disordered ice VII (highly ionized ice VII, see also Ref. 10) and proton-disordered symmetric ice X, which are featured by proton tunneling and zero-point motion, respectively (see Ref. 4). Its structure can be described by a space group $Pn3m$ as well as fully centered ice X. These two regimes of ice X are crystallographically difficult to be distinguished. We, therefore, referred generally the two regimes of ice X as ice X. The translationally disordered ice X is an intermediate ionized phase between molecular ice phases (VII, VIII) and the fully centered ice X (atomic phase).

[8] Ph. Pruzan, J.C. Chervin, and B. Canny, J. Chem. Phys. **99**, 9842 (1993).

[9] The ice VIII-X phase transition (or boundary) is the phase transition (or boundary) from molecular ice VIII to nonmolecular ice X, and is the same in meaning as the phase transition (or boundary) from ice VIII to the translationally disordered ice X in this

paper. The ice VIII-X transition (or boundary) can be understood in the same way.

[10] Ph. Pruzan, J. Mol. Struct. **322**, 279 (1994).

[11] Ph. Pruzan, E. Wolanin, M. Gauthier, J.C. Chervin, and B. Canny, D. Hausermann, and M. Hanfland, J. Phys. Chem. B **101**, 6230 (1997).

[12] R.J. Hemley, A.P. Jephcoat, H.K. Mao, C.S. Zha, L.W. Finger, and D.E. Cox, Nature (London) **330**, 737 (1987).

[13] E. Wolanin, Ph. Pruzan, J.C. Chervin, B. Canny, M. Gauthier, D. Hausermann, and M. Hanfland, Phys. Rev. B **56**, 5781 (1997).

[14] P. Loubeyre, R. LeToullec, E. Wolanin, M. Hanfland, and D. Hausermann, Nature (London) **397**, 503 (1999).

[15] J. Hama and K. Suito, Phys. Lett. A **187**, 346 (1994).

[16] W.B. Holzapfel, Physica B **265**, 113 (1999).

[17] K. Aoki, H. Yamawaki, M. Sakashita, and H. Fujihisa, Phys. Rev. Lett. **76**, 784 (1996).

[18] A.F. Goncharov, V.V. Struzhkin, M.S. Somayazulu, R.J. Hemley, and H.K. Mao, Science **273**, 218 (1996).

[19] K. Aoki, H. Yamawaki, M. Sakashita, and H. Fujihisa, Phys. Rev. B **54**, 15 673 (1996).

[20] V.V. Struzhkin, A.F. Goncharov, R.J. Hemley, and H.K. Mao, Phys. Rev. Lett. **78**, 4446 (1997).

[21] M. Song, H. Yamawaki, H. Fujihisa, M. Sakashita, and K. Aoki, Phys. Rev. B **60**, 12 644 (1999).

[22] Eriko Katoh, M. Song, H. Yamawaki, H. Fujihisa, M. Sakashita, and K. Aoki, Phys. Rev. B **62**, 2976 (2000).

[23] A.F. Goncharov, V.V. Struzhkin, H.K. Mao, and R.J. Hemley, Phys. Rev. Lett. **83**, 1998 (1999).

[24] J.C. Chervin, B. Canny, M. Gauthier, and Ph. Pruzan, Rev. Sci. Instrum. **64**, 203 (1993).

[25] H.K. Mao, J. Xu, and P.M. Bell, J. Geophys. Res., [Atmos.] **91**, 4673 (1986).

[26] K.R. Hirsch and W.B. Holzapfel, J. Chem. Phys. **84**, 2771 (1986).

[27] W.B. Holzapfel, B. Seiler, and M. Nicol, J. Geophys. Res. **89**, B706 (1984).

[28] R.J. Nelmes, J.S. Loveday, W.G. Marshall, G. Hamel, J.M. Besson, and S. Klotz, Phys. Rev. Lett. **81**, 2719 (1998).

[29] J.M. Besson, S. Klotz, G. Hamel, W.G. Marshall, R.J. Nelmes, and J.S. Loveday, Phys. Rev. Lett. **78**, 3141 (1997).

[30] R.J. Nelmes, J.S. Loveday, R.M. Wilson, J.M. Besson, Ph. Pruzan, S. Klotz, G. Hamel, and S. Hull, Phys. Rev. Lett. **71**, 1192 (1993).

[31] J.S. Tse and D.D. Klug, Phys. Rev. Lett. **81**, 2466 (1998).

[32] E. Whalley, in *The Hydrogen Bond*, edited by P. Schuster, G. Zundel, and C. Sandorfy (North-Holland, Amsterdam, 1976), p. 1425.

[33] M.G. Sceats and S.A. Rice, in *Water, a Comprehensive Treatise*, edited by F. Franks (Plenum, New York, 1982), Vol. 7, p. 83.

[34] P.T.T. Wong and E. Whalley, J. Chem. Phys. **64**, 2359 (1976).

[35] S.P. Tay, D.D. Klug, and E. Whalley, J. Chem. Phys. **83**, 2708 (1985).

[36] M. Bernasconi, P.L. Silvestrelli, and M. Parrinello, Phys. Rev. Lett. **81**, 1235 (1998).

[37] M. Benoit, D. Marx, and M. Parrinello, Solid State Ionics **125**, 23 (1999).

[38] Here we assume that the O-D bond length in D_2O ice is the same as the O-H bond length in H_2O ice. No evidence shows that deuteration significantly alters hydrogen bond length in ice. The hydrogen-bonded O-O distance in D_2O ice can be taken as the same as in H_2O ice (see Ref. 13).